第 29 卷第 10 期 无 机 化 学 学 报 Vol.29 No.10
2013 年 10 月 CHINESE JOURNAL OF INORGANIC CHEMISTRY 2257-2264

EDTA 辅助水热法制备性能优异的棒状 $LiFePO_4$/C 材料

董 静[1] 钟本和[1] 钟艳君[1] 唐 艳[1] 刘 恒[2] 郭孝东*,[1]
([1]四川大学化学工程学院,成都 610065)
([2]四川大学材料科学与工程学院,成都 610065)

摘要:以乙二胺四乙酸为配位剂采用水热法制备了棒状 $LiFePO_4$/C 材料。采用 X 射线衍射、扫描电镜、透射电镜、循环伏安、交流阻抗和恒电流充放电测试等对材料进行表征。结果表明:乙二胺四乙酸对材料的形貌和电性能均有很大影响。通过加入乙二胺四乙酸,材料的形貌由不规则的颗粒变为棒状的颗粒且颗粒的厚度由 140~200 nm 减少至 40~90 nm,材料的表面包覆约 3.5 nm 的均匀碳层,且该材料极化较小且界面阻抗较低。0.1C 放电比容量为 167 mAh·g^{-1}(接近理论容量 170 mAh·g^{-1})。

关键词:材料科学;水热法;循环伏安;锂电池;$LiFePO_4$;乙二胺四乙酸
中图分类号:O646;TM912.9 **文献标识码**:A **文章编号**:1001-4861(2013)10-2257-08
DOI:10.3969/j.issn.1001-4861.2013.00.333

EDTA-Assisted Hydrothermal Synthesis for Rod-Like $LiFePO_4$ with Enhanced Electrochemical Properties

DONG Jing[1] ZHONG Ben-He[1] ZHONG Yan-Jun[1] TANG Yan[1] LIU Heng[2] GUO Xiao-Dong*,[1]
([1]*College of Chemical Engineering, Sichuan University, Chengdu* 610065, *China*)
([2]*College of Materials Science and Engineering, Sichuan University, Chengdu* 610065, *China*)

Abstract: Rod-like $LiFePO_4$ was synthesized by hydrothermal method using ethylene diamine tetraacetic acid (EDTA) as complexing agent to control the growth of the crystal. The materials were characterized by X-ray diffraction (XRD), scanning electron microscopy (SEM), transmission electron microscope (TEM), cyclic voltammetry (CV), electrochemical impedance spectroscopy (EIS) and galvanostatic charge-discharge test. The results show that EDTA has great influence on the morphology and electrochemical performance. The crystal morphology develops from irregular particles to rod-like particles and the thickness of the particles decreases from 140~200 nm to 40~90 nm by adding EDTA and the obtained $LiFePO_4$/C with EDTA exhibits a homogenous carbon coating layer with a thickness of ~3.5 nm. The discharge capacity is 167 mAh·g^{-1} (close to the theoretical capacity of 170 mAh·g^{-1}) at 0.1C. The CV and EIS results indicate the samples prepared with EDTA have a lower polarization and lower interfacial resistance.

Key words: materials science; hydrothermal synthesis; voltammetry; lithium ion batteries; lithium iron phosphate; ethylene diamine tetraacetic acid

Since the pioneering work of Padhi et al.[1], the olivine-type phosphates $LiFePO_4$ has received extensive attention with respect to its application as a cathode material in rechargeable Li-ion batteries, owing to its high theoretical capacity (170 mAh·g^{-1}), low cost, environmental benign and high safety. In

收稿日期:2013-03-21。收修改稿日期:2013-05-17。
四川大学青年基金(No.2011SCU11081);教育部高校博士学科点科研基金(No.20120181120103)资助项目。
*通讯联系人。E-mail:xiaodong2009@scu.edu.cn

addition, $LiFePO_4$ has good cycle stability and a flat discharge potential of 3.45 V versus Li^+/Li. Despite the above mentioned advantages, the main obstacles for $LiFePO_4$ are its intrinsic low electronic conductivity ($\sim10^{-9}$ $cm^2\cdot s^{-1}$) [2] and low lithium ion diffusivity ($\sim10^{-18}$ $cm^2\cdot s^{-1}$)[3]. Great progress has been made to improve the performances and synthesis techniques of $LiFePO_4$ up to now. To eliminate the impediments of $LiFePO_4$ materials, numerous approaches have been reported, such as coating different conductive materials (conductive carbon or polymers)[4-5], minimizing the particle size [6-8] and doping with supervalence cation [9]. Furthermore, numerous synthetic strategies have been developed to synthesize $LiFePO_4$, such as co-precipitation, solid-state reactions, sol-gel, solvothermal and hydrothermal method. Among them, the hydrothermal synthesis of $LiFePO_4$ is a promising method due to its narrow particle size distribution, fast reaction rate and facile size control.

Owing to the importance of particle shape on the performance of $LiFePO_4$, lots of studies have been devoted to the preparation of olivine $LiFePO_4$ with various morphologies and reduced particle size in hydrothermal method. For instance, Fei Teng et al. synthesized $LiFePO_4$ nanodendrites in the ethylene glycol/water (EG/W) system using dodecyl benzene sulphonic acid sodium (SDBS) as the surfactant[10] and developed to fabricate $LiFePO_4$ nanorod arrays using anodic aluminum oxide (AAO) as the template[11]. Lu et al. [12]. reported that $LiFePO_4$ with a variety of unusual morphologies was prepared in the presence of ammonium ions and citric acid. Dinesh Rangappa et al. [13] synthesized hierarchical flower-like $LiFePO_4$ using ethylene glycol as the solvent with oleic acid and hexane as the surfactant and co-solvent. In general, the primary approaches to prepare well-defined morphology and smaller particle size in hydrothermal method are using organic solvent or template, which make the preparation process more complex and more expensive. We report here a simple, quick and low cost hydrothermal synthesis only using EDTA as the complexing agent and dispersing agent to prepare the defined morphology with reduced particle size. The obtained rod-like $LiFePO_4$ exhibits narrow particle size distribution and better electrochemical properties.

1 Experimental

1.1 Synthesis of $LiFePO_4$/C

All the reactants were of analytical grade and used without further purification. In a typical synthesis, 0.3 mol H_3PO_4, 0.3 mol $FeSO_4\cdot7H_2O$ and 0.9 mol $LiOH\cdot H_2O$ were dissolved in deionized water, respectively. First, the lithium source and phosphorus source were blended under magnetic stirring, and then $FeSO_4$ solution slowly added to the above solution to keep the molar ratio n_{Li}:n_{Fe}:n_P=3:1:1. Finally, 0.03 mol EDTA was added to the obtained solution. After that, the resulting mixture was transferred into a 2L-capacity Teflon-lined stainless steel autoclave, and then heated at 180 ℃ for 10 h. After being cooled to room temperature, the product was centrifuged, washed several times with absolute alcohol and distilled water and then dried in a vacuum oven at 90 ℃ for 12 h. For further carbon coating on $LiFePO_4$ nanostructures, the powders after drying mentioned above were mixed with glucose (20wt%) as a carbon source by planetary ball milling, and then the blend was calcined at 700 ℃ for 5 h in an inert atmosphere. In order to confirm the influence of EDTA on the products, a control experiment was also carried out. The $LiFePO_4$/C materials prepared with EDTA and without EDTA were denoted as sample A and B.

1.2 Materials characterization

The phase structures of the samples were investigated by X-ray diffraction (XRD, D/max-rB, Rigaku, Cu $K\alpha$ radiation) (λ=0.154 18 nm, 40 kV, 40 mA, scintillation counter, scanning range (2θ): 10°~70°, step scanning: 0.5°·min^{-1}). The morphology and particle size of the prepared nanocrystals were observed by scanning electron microscopy (HITACHI S-4800). The microstructure and the surface texture of crystal were observed by transmission electron microscopy (JEM-2100) operated at 200 kV acceleration voltage. The particle size distribution was estimated by laser particle size distribution tester (JL-

1155). The electronic conductivities of the samples were measured by a four-point probe method (KDY-1). The cyclic voltammetry tests and electrochemical impedance spectroscopy were performed on electrochemical workstation (CHI660B). The carbon content was measured by analytical instrument (CS-902).

1.3 Electrochemical characterization

The positive slurry was prepared with 80wt% active material, 13wt% acetylene black (conducting additive), 7wt% polyvinylidene fluoride (PVDF, binder) and N-methylpyrro lidone (NMP, solvent). The slurry was spread uniformly onto a thin aluminum foil, dried in vacuum at 100 ℃ for 16 h and then cut into pieces. The formed cathode was assembled into a CR2032 button battery in an argon-filled glove box, with Li anode, 1 $mol \cdot L^{-1}$ $LiPF_6$ in a mixed solvent of ethylene carbonate (EC) and dimethyl carbon (DMC) (V_{EC}:V_{DMC}=1∶1) electrolyte and a Celgard-2400 separator. The electrochemical performance of the cells was tested by a high precision battery performance testing system. The cells were galvanostatically charged and discharged at room temperature between 2.5 and 4.3 V versus Li^+/Li.

2 Results and discussion

2.1 Structure and morphology analysis

Fig.1 shows the XRD patterns of precursors prepared with and without EDTA. The precursors were the precipitation prepared from the mixing of the raw materials. It is found that there is no obvious difference between the two precursors. All main characteristic peaks of the two precursors are coincided with the diffraction peaks of $Fe_3(PO_4)_2 \cdot 8H_2O$ (PDF# 30-0662) and Li_3PO_4 (PDF# 25-1030) without any obvious impurity phase. The results are consistent with previous reports[14-15] that $Fe_3(PO_4)_2 \cdot 8H_2O$ and Li_3PO_4 must be the intermediate in the formation of $LiFePO_4$. These observed results clearly indicate Fe-EDTA is not in the precursors, maybe it is dissolved and then not in the precursor or it could not be characterized by XRD.

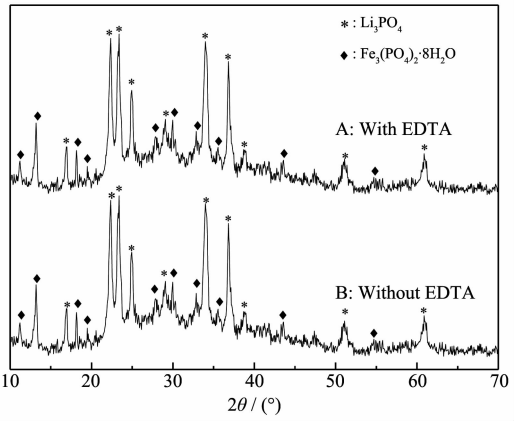

Fig.1　XRD patterns of precursors prepared with EDTA and without EDTA

The XRD patterns of $LiFePO_4$/C composites are displayed in Fig.2. All the diffraction peaks in the XRD patterns could be indexed to an orthorhombic space group, Puma (PDF# 83-2092). The XRD pattern clearly shows the single-phase formation of $LiFePO_4$ without any observable impurity phases (such as $Fe_3(PO_4)_2$, Li_3PO_4, FeP). It demonstrates that the introduction of complexing agent does not change the sample′s crystal structure. Additionally, the intensity of all the diffraction peaks of sample A is stronger than sample B. This suggests that using EDTA as complexing agent is favorable for increasing the crystallinity of the $LiFePO_4$. The obtained lattice parameters are (a) a=1.029 656 nm, b=0.598 161 nm, c=0.467 506 nm with a cell volume of 0.287 94 nm^3; (b) a=1.029 92 nm, b=0.598 68 nm, c=0.467 26 nm with a cell volume of 0.288 11 nm^3 for the two $LiFePO_4$/C samples with EDTA (a) and without EDTA (b), respectively. It is clear that sample A owns smaller cell volume, which may be related to a better crystallinity with EDTA as complexing agent. These values are comparable with those reported earlier in

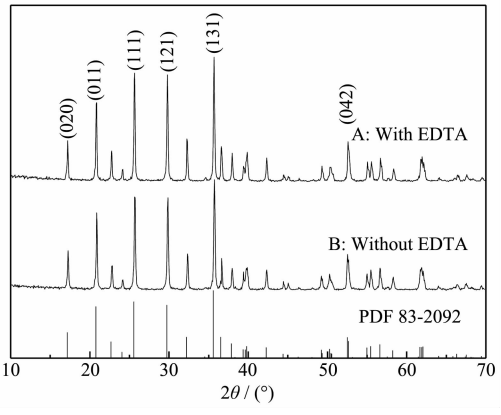

Fig.2　XRD patterns of sample A and sample B

the literatures[16-17].

There is no carbon observed in the XRD patterns, because the residual carbon decomposed from glucose and EDTA is amorphous in the $LiFePO_4$/C composite[18]. The carbon content of $LiFePO_4$/C obtained with EDTA is 5.5% and another sample is 5.2%. Clearly, EDTA is not washed off completely during the filtering process. This can be ascribed to the remnant carbon after the pyrolysis of EDTA. Therefore, the carbon content of the sample A is a little more than that of sample B.

Fig.3 shows the SEM images of $LiFePO_4$/C. By adding EDTA, rod-like $LiFePO_4$ is obtained, otherwise only irregular particles are prepared and the size of sample B is much larger than that of sample A. It demonstrates that EDTA chelation-assisted hydrothermal method can effectively decrease the particle size and control the morphology. As reported in the literatures[18-20], EDTA has been widely used as chelating agent and structure-directing template. The chelating role of EDTA group in the synthesis process is to greatly control the concentration of Fe^{2+}, thus to modulate the growth rate of $LiFePO_4$ crystallite. Therefore, the use of EDTA can effectively decrease the crystal size and modulate the crystal growth to obtain the defined shape.

The particle size distribution of sample A and sample B is shown in Fig.4. Sample A presents unimodal distribution, but bimodal distribution for sample B. The peak located between 10~100 μm is absence for sample A. As reported in the literature[21], EDTA has the function of dispersive action. Furthermore, the peak value of 0.1~1 μm for sample A is bigger than sample B, which coincides with the results of SEM. It indicates that adding EDTA in hydrothermal method can effectively reduce the particle agglomeration.

The morphology and microstructure of the rod-like $LiFePO_4$ obtained with EDTA were further characterized by TEM, high resolution TEM (HRTEM) and the selected area electron diffraction (SAED) images. Fig.5a presents the typical TEM image of

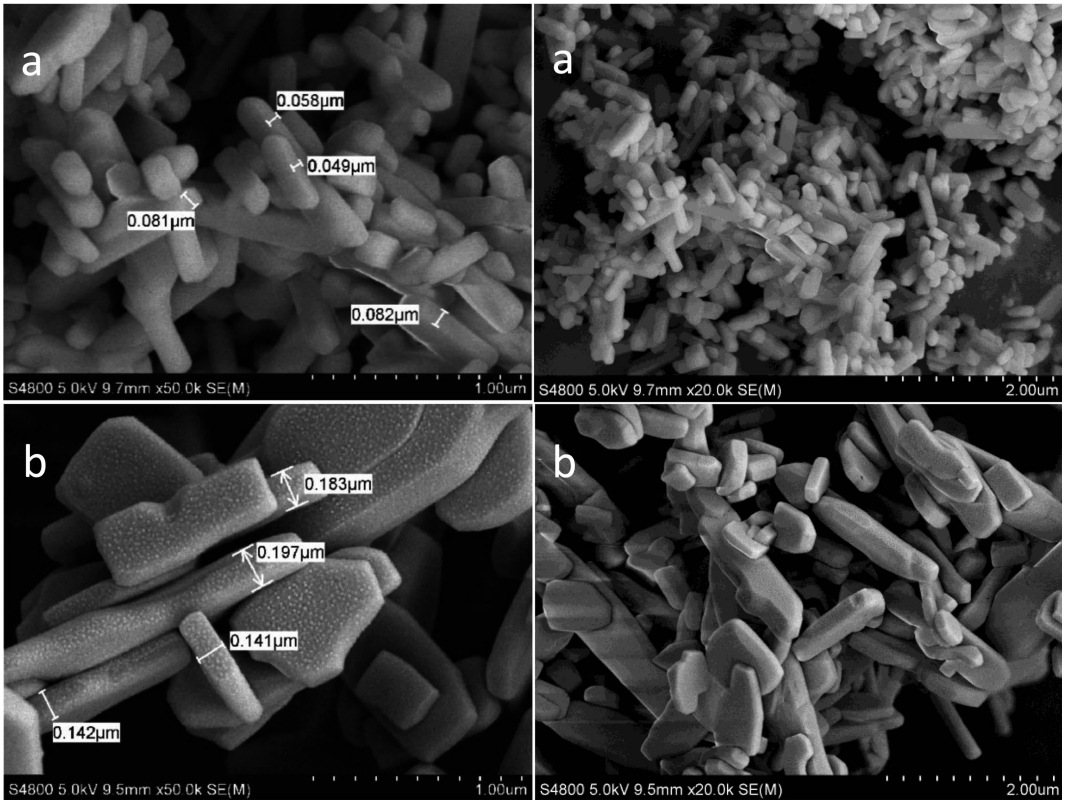

(a) Sample A; (b) Sample B

Fig.3 SEM images of $LiFePO_4$/C

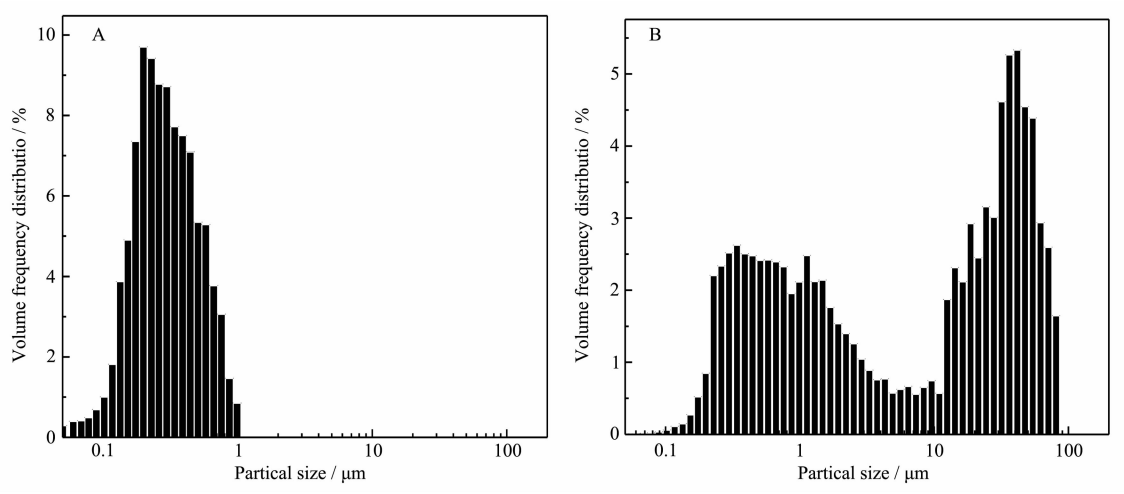

Fig.4　Particle size distribution of sample A and sample B

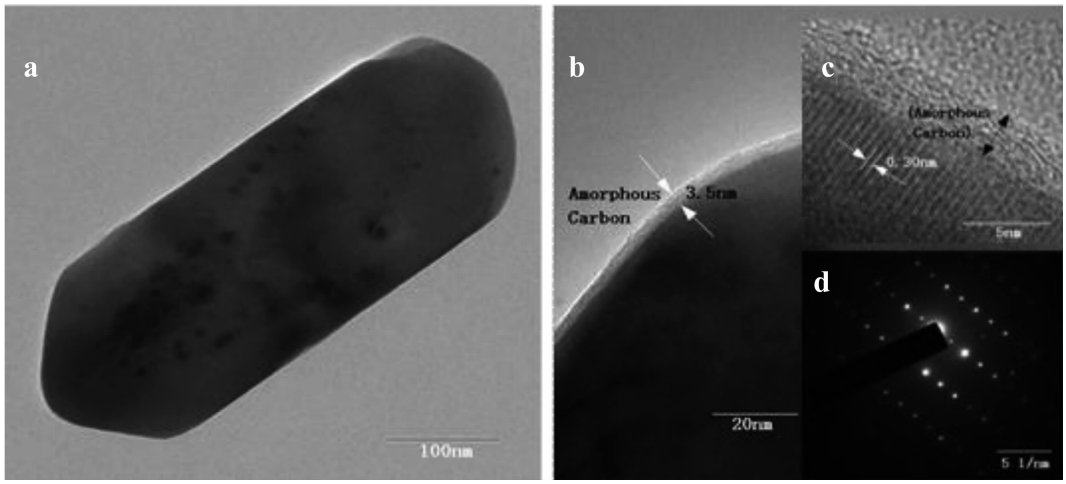

Fig.5　TEM, HRTEM image and SAED of $LiFePO_4$/C obtained with EDTA

$LiFePO_4$/C. The morphology of the particles is nano-sized rods, which is in good agreement with the above SEM observations. Fig.5b shows that an armorphous carbon coating layer with a thickness of ~3.5 nm is homogenously distributed on the $LiFePO_4$ particles, the uniform carbon layer is beneficial to improve the conductivity of the material. The HRTEM image displays clear crystal lattices with *d*-spacing of 0.30 nm, corresponds to the (020) plane of $LiFePO_4$ (Fig. 5c). The SAED pattern in Fig.5d with clear lattice fringes suggests that the good crystalline $LiFePO_4$ nanostructures are formed under hydrothermal conditions by adding EDTA.

2.2　Electrochemical measurements

Fig.6a presents the galvanostatic charge/discharge curves of sample A and sample B measured at 0.1C in the potential range of 2.5 to 4.3 V. Both the samples possess a flat plateau around 3.4 V, which corresponds to the redox couple of Fe^{3+}/Fe^{2+}. Sample A delivers a higher discharge capacity of 167 $mAh \cdot g^{-1}$, but sample B presents a discharge capacity of 150 $mAh \cdot g^{-1}$. Meanwhile, sample B display a wider space of the charge-discharge voltage profiles than sample A, which indicates that sample A may possess lower electrode polarization and higher reversible capacity at a higher rate. Fig.6b shows the rate capability of sample A and B. The discharge capacities of sample A are 167, 157, 147, 134, 120, 101, 79 $mAh \cdot g^{-1}$ at 0.1C, 0.2C, 0.5C, 1C, 3C, 5C and 10C, respectively, and sample B is 150, 139, 121, 90, 65, 45, 23 $mAh \cdot g^{-1}$ at 0.1C, 0.2C, 0.5C, 1C, 3C, 5C and 10C, respectively. It is obvious that sample A shows a higher capacity at every testing rate than sample B. The electronic conductivity of $LiFePO_4$/C

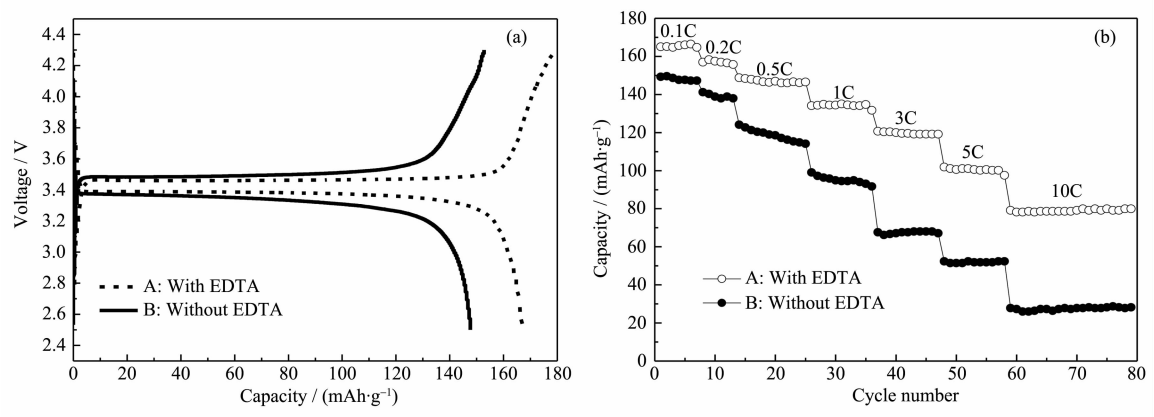

Fig.6 (a) Charge/discharge curves of A and sample B; (b) Rate performance of sample A and sample B

materials obtained with EDTA is 1.18×10^{-2} S·cm^{-1} and the $LiFePO_4$/C materials obtained without EDTA is 8.13×10^{-3} S·cm^{-1} as measured by a four-point probe method. The better electrochemical properties of the sample A could be attributed to its smaller particle size and the less particle agglomeration. This is because the smaller particle size shortens the distance of the transport passage, and increases the conductivity of the sample. Therefore, electrochemical performance of $LiFePO_4$/C material can be effectively improved by adding EDTA.

The first five cyclic voltammogram curves of $LiFePO_4$/C composite in the voltage range of 2.5~4.3 V at a constant scanning rate of 0.1 mV·s^{-1} are shown in Fig.7. The voltage charge/discharge profiles of all five cycles are almost reduplicative, suggesting the good reversibility of lithium extraction/insertion reactions in the $LiFePO_4$/C composites prepared through hydrothermal method. In the CV plots of $LiFePO_4$ cathode material, the higher and sharper

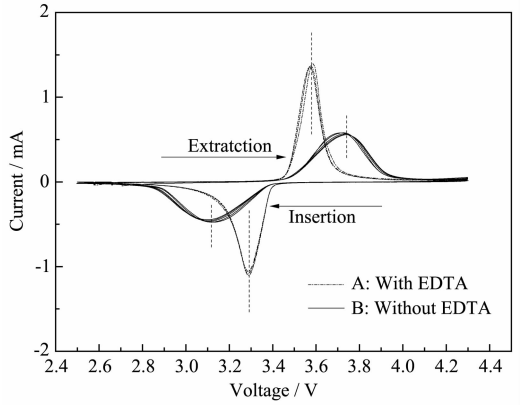

Fig.7 CV curves of sample A and sample B at a scan rate of 0.1 mV·s^{-1}

current peaks and the smaller charge and discharge voltage plateaus difference imply better electrode reaction kinetics and better rate performance[23]. The CV curves of sample A show more symmetrical and sharper shape of the anodic/cathodic peaks, which indicates an improvement in the kinetics of the lithium insertion/extraction at the electrode/electrolyte interface[22-23]. In contrast, sample B electrode has lower peaks in CV curves. Furthermore, the higher peak voltage separation of sample B indicates that electrochemical kinetics could be strongly inhibited and that high polarization overpotential is present. Thus, sample A shows better electrochemical property. The result is in coincidence with the electrochemical measurements.

Fig.8 presents the Nyquist curves of the two samples and an equivalent circuit fitted by Zview2.0 program. An intercept at the Z_{real} axis in high frequency corresponds to the Ohmic resistance (R_Ω), which represents the resistance of the electrolyte. The diameter of the semicircle on the Z_{real} axis is approximately equal to the charge transfer resistance (R_{ct}). The inclined line in the lower frequency represents the Warburg impedance, which is associated with lithium-ion diffusion in the $LiFePO_4$ particles[24]. The lithium-ion diffusion coefficient (D_{Li}) could be calculated using the formula **1**[25]. Formula **1**:

$$D_{Li}=\frac{R^2T^2}{2A^2n^4F^4C^2\sigma^2}$$

where R is the gas constant, T is the absolute temperature, A is the surface area of the cathode, n is

the number of electrons per molecule during oxidization, F is the Faraday constant, C is the concentration of lithium ion (7.69 mol·L^{-1}), and σ is the Warburg coefficient. The Warburg coefficient σ is calculated by the linear fitting result of Z' and $\omega^{-1/2}$ from the EIS data. All the parameters obtained and calculated from EIS are shown in Table 1. It is obvious that the R_{ct} drastically decreases and lithium-ion diffusion coefficient increases for sample A. The reasons can be explained in terms of particle size, as reported previously [26], because small particle can shorten the distance of the transport distance.

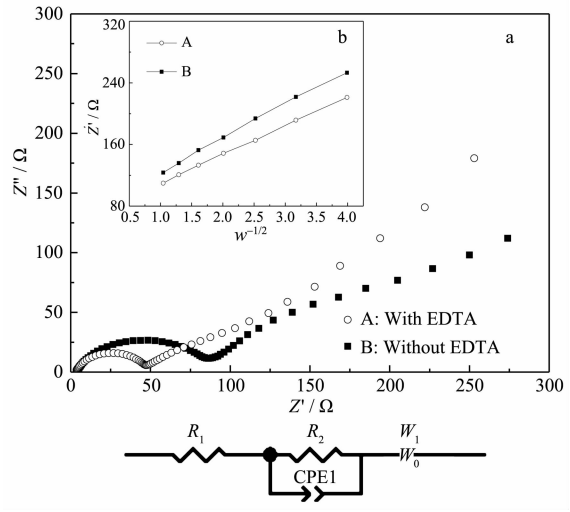

Fig.8　(a) Electrochemical impedance spectra of sample A and sample B; (b) Relationship plot between Z' and $\omega^{-1/2}$ at low-frequency region

Table 1　Impedance parameters of $LiFePO_4$/C cells (A with EDTA B without EDTA)

Sample	R_Ω / Ω	R_{ct} / Ω	σ	D_{Li} / (cm^2·s^{-1})
A	2.777	38.55	37.5	1.90×10^{-13}
B	2.85	52.29	44.2	1.36×10^{-13}

3　Conclusions

In summary, we propose a simple, quick and low cost hydrothermal synthesis route to control the morphology of $LiFePO_4$/C only by adding EDTA, rather than by changing the temperature, pH value, concentration or solvent. The prepared $LiFePO_4$/C with EDTA presents a well-crystallized nanorod structure and coated with carbon layer of ~3.5 nm. The chelating role of EDTA group in the synthesis process is to greatly control the concentration of Fe^{2+}, and to modulate the growth rate of $LiFePO_4$ crystallite. Therefore, rod-like $LiFePO_4$ with reduced size is obtained, otherwise only irregular particles are prepared. Moreover, EDTA has the function of dispersive action and then restraints the sample′s aggregation. The $LiFePO_4$/C obtained with EDTA exhibits excellent reversible capacities at galvanostatic charge-discharge test. The specific discharge capacities have been reached 167, 157, 147, 134, 120, 101, 79 mAh·g^{-1} at 0.1C, 0.2C, 0.5C, 1C, 3C, 5C and 10C, respectively. The significantly improved electrochemical performances of the material could be attributed to the larger proportion of nano-sized particles which is originated from EDTA as chelating agent and dispersing agent.

Acknowledgements: This work was supported by the Sichuan University Funds for Young Scientists (2011SCU11081), and the Research Fund for the Doctoral Program of Higher Education, the Ministry of Education (20120181120103).

References:

[1] Padhi A K, Nanjundaswamy K S, Goodenough J B. *J. Electrochem. Soc.*, **1997**,**144**(4):1188-1194

[2] Chung S Y, Chiang Y M. *Electrochem. Solid-State Lett.*, **2003**,**6**:A278-A281

[3] Srinivasan V, Newman J. *J. Electrochem. Soc.*, **2004**,**151**:A1517-A1529

[4] Chen Z H, Dahn J R. *J. Electrochem. Soc.*, **2002**,**149**:A1184-A1189

[5] Wilcox J D, Doeff M M, Marcinek M, et al. *J. Electrochem. Soc.*, **2007**,**154**:A389-A395

[6] WANG Xiao-Juan(王小娟), LI Xin-Hai(李新海), WANG Zhi-Xing(王志兴), et al. *J. Funct. Mater.*(*Gongneng Cailiao*), **2009**,**40**(12):1996-2003

[7] YU Hong-Ming(于红明), ZHENG Wei(郑威), CAO Gao-Shao(曹高劭), et al. *Acta Phys.-Chim. Sin.*(*Wuli Huaxue Xuebao*), **2009**,**25**(11):2186-2190

[8] XU Rui(徐瑞), ZHONG Ben-He(钟本和), GUO Xiao-Dong(郭孝东) et al. *Chinese J. Inorg. Chem.*(*Wuji Huaxue Xuebao*), **2012**,**28**(7):1506-1512

[9] TANG Hong(唐红), GUO Xiao-Dong(郭孝东), TANG Yan(唐

艳), et al. *Chinese J. Inorg. Chem.*(*Wuji Huaxue Xuebao*), **2012**,**28**(4):809-814

[10]Teng F, Santhanagopalan S, Lemmens R, et al. *Solid State Sci.*, **2010**,**12**:952-955

[11]Lu Z G, Chen H L, Robert R, et al. *Chem. Mater.*, **2011**,**23**: 2848-2859

[12]Rangappa D, Sone K, Kudo T, et al. *J. Power Sources*, **2010**,**195**:6167-6171

[13]Lee M H, Kim J Y, Song H K. *Chem. Commun.*, **2010**,**46**: 6795-6797

[14]He L H, Zhao Z W, Liu X H, et al. *Trans. Nonferrous Met. Soc. China*, **2012**,**22**:1766-1770

[15]Saravanan K, Balaya P, Reddy M V, et al. *Energy Environ. Sci.*, **2010**,**3**:457-464

[16]Wang Z L, Su S R, Yu C Y, et al. *J. Power Sources*, **2008**, **184**:633-636

[17]Li C F, Hua N, Wang C Y, et al. *J. Solid State Electrochem.*, **2011**,**15**:1971-1976

[18]Zhu Z F, Du J, Li J Q, et al. *Ceram. Int.*, **2012**,**38**:4827-4834

[19]Ha J H, Muralidharan P, Kim D K. *J. Alloys Compd.*, **2009**, **475**:446-451

[20]Adldinger H K, Calnek B W. *Archiv Für Die Gesamte Virusforschung*, **1971**,**34**:391-395

[21]Lan Y C, Wang X D, Zhang J W, et al. *Powder Technol.*, **2011**,**212**:327-331

[22]Dimesso L, Spanheimer C, Jacke S, et al. *J. Power Sources*, **2011**,**196**:6729-6734

[23]Shin H C, Cho W I, Jang H. *Electrochim. Acta*, **2006**,**52**: 1472-1476

[24]Yang K R, Deng Z H, Suo J S, *J. Power Sources*, **2012**,**201**: 274-279

[25]Kwon S J, Kim C W, Jeong W T, et al. *J. Power Sources*, **2004**,**137**:93-99